ISSN (Print) 1226-1750
ISSN (Online) 2233-6656
Journal of Magnetics 27(4), 356-365 (2022) https://doi.org/10.4283/JMAG.2022.27.4.356

A Study on the Suitability of High Space Factor Wire for Traction Motors

Ju-Hyeong Moon[1], Dong-Yeol Lee[1], and Dong-Woo Kang[2]*

[1]*Dept. of Electronic and Electrical Engineering, Keimyung University, Daegu 42601, Republic of Korea*
[2]*Dept. of Electrical Energy Engineering, Keimyung University, Daegu 42601, Republic of Korea*

(Received 13 September 2022, Received in final form 6 October 2022, Accepted 7 October 2022)

Recently, the method of designing motors according to the high voltages of vehicle systems has been reestablished; in the case of traction motors for electric vehicles (EVs), which are large devices, hairpin winding structures have been increasingly adopted for improved outputs and efficiencies. However, for hairpin windings, significant AC losses can occur in EV systems requiring high driving speeds, thereby decreasing the efficiencies in high-speed operation regions. Therefore, this study designs a motor that uses a round wire winding and a hairpin winding under the same vehicle system conditions and analyzes the suitability of the hairpin structure for application to an EV traction motor under the current vehicle system condition.

Keywords : electric vehicle, traction motor, hair-pin wire, AC resistance

1. Introduction

Recently, the demand for electric vehicles (EVs) has rapidly increased. In addition, as the system voltages of vehicles increase, studies on the design of motors for high-voltage vehicles are required. Typically, traction motors must be designed to have high outputs and efficiencies, and their design may be closely related to the development of high-performance permanent magnet manufacturing and material technologies such as those involved in the development of self-bonding cores. In addition, winding wires are related to the performance of motors, and studies to improve the cooling performance and increase the slot fill factor are currently underway [1-4]. Recently, with the increase in the voltages of vehicle systems, hairpin windings have been increasingly adopted. A hairpin wire uses a structure in which the windings are stacked inside the slot, the contact surface with the core is wide, and the dead space is small; such structures are advantageous for cooling and improving the slot fill factor. However, because the use of strands is often difficult, thick and large wires must be used in traction motors for EVs. In the case of a traction motor for a vehicle using a gear, a high driving speed is required. Moreover, if thick and large wires are used, the AC resistance owing to the skin effect at high speed increases [5-7]. Based on previous studies, a thin wire should be used to minimize skin effects. However, when manufacturing a motor with a hairpin structure, the upper and lower ends of the winding must be twisted, but this may expose the winding to a risk of breakdown [8]. Therefore, a relatively thick wire must be used, but AC resistance loss owing to the skin effect occurs significantly during high-speed operation. In addition, the suitability of the hairpin winding should be reviewed as the speed of the traction motor increases, such as in multi-stage reducers. This study compares the AC resistance ratios according to the shape of the round and square wires of the traction motor. In addition, we design a motor using each hairpin and round wire winding under the same vehicle system conditions and examine whether the hairpin structure is suitable for a traction motor in the current vehicle system condition by comparing characteristics in the driving area.

2. AC Resistance Loss in Wires

Numerous studies on AC resistance loss are underway [9-13]. In this study, the resistive loss caused by a high-frequency current is called AC resistive loss. Generally, the wire of a motor driven at high speed is divided into strands. Because the number of poles, driving speed, and frequency of the input current are proportional, the skin effect occurs in the wire, and the penetration depth is expressed as

©The Korean Magnetics Society. All rights reserved.
*Corresponding author: Tel: +82-10-3632-0403
Fax: +82-53-580-5441, e-mail: dwkang1222@gmail.com

© 2022 Journal of Magnetics

$$\delta_{skin} = \frac{1}{\sqrt{\pi f \mu_r \mu_0 \sigma}} \tag{1}$$

where δ_{skin} is the penetration depth according to the frequency of the applied current, f is the frequency of the applied current, $\mu_r\mu_0$ is the magnetic permeability of the wire, and σ is the conductivity. As the driving speed increases, the penetration depth owing to the skin effect decreases, and the effective cross-sectional area through which the current can flow decreases. Therefore, the resistance owing to the skin effect is

$$R = \frac{l_c}{\sigma S_c} \therefore S_c = \begin{cases} \pi r_c^2 - \pi(r_c - \delta_{skin})^2 & r_c > \delta_{skin} \\ \pi r_c^2 & r_c > \delta_{skin} \end{cases} \tag{2}$$

where R is the resistance of the wire, S_c is the effective cross-sectional area of the wire, r_c is the radius of the wire, and l_c is the total length of the wire. The reduction in the effective cross-sectional area owing to the skin effect increases the resistance and loss. Therefore, when designing a high-speed multipole machine, the diameter of the winding is designed to be smaller than the penetration depth; thus, strands are used to wind the wire.

The shape parameters of the winding inside the stator slot are shown in Fig. 1. The AC resistance loss ratio of the hairpin winding is expressed as

$$k_R = \frac{R_{AC}}{R_{DC}} \tag{3}$$

where k_R is the ratio of the DC to AC resistance. The effective thickness of the conductor in Fig. 1 according to (1) is expressed as

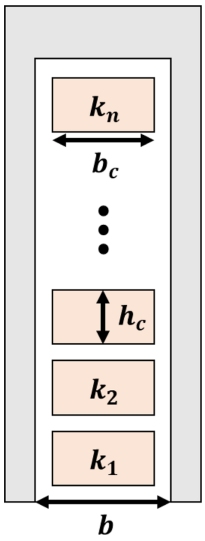

Fig. 1. (Color online) Shape of the wire in the stator slot.

$$\xi = \alpha h_{c0} = h_{c0}\sqrt{\frac{1}{2}\omega\mu_0\sigma_c\frac{b_{c0}}{b}} \tag{4}$$

where ξ is the effective thickness of the conductor, h_{c0} is the height of the conductor, ω is the angular velocity, σ_c is the conductivity of the conductor, b_{c0} and b are the widths of the conductor and slot, respectively.

The resistance coefficient of the k-th layer is provided by ignoring the insulation thickness between the winding and the winding with a constant width of the conductor in the slot.

$$k_{Rk} = \varphi(\xi) + k(k-1)\psi(\xi) = \xi\frac{\sinh 2\xi + \sin 2\xi}{\cosh 2\xi - \cos 2\xi} \tag{5}$$

$\varphi(\xi)$ and $\psi(\xi)$ are expressed as

$$\varphi(\xi) = \xi\frac{\sinh 2\xi + \sin 2\xi}{\cosh 2\xi - \cos 2\xi} \tag{6}$$

$$\psi(\xi) = 2\xi\frac{\sinh\xi - \sin\xi}{\cosh\xi + \cos\xi} \tag{7}$$

The average resistance coefficient k_R of each conductor can be approximated as [14, 15].

$$k_R = \varphi(\xi) + \frac{k_n^2 - 1}{3}\psi(\xi) \tag{8}$$

Equation (8) is the AC resistance coefficient of the model with winding layers, as defined by Dowell. From (5), the AC resistance coefficient increases as the conductor approaches the slot opening. The AC resistance ratio for each winding aspect ratio is shown in Fig. 2. The AC resistance loss increases when the number of poles and operating speed increase and the conductor is thick.

3. Model Design and analysis

Table 1 lists the motor design specifications based on an SUV-class vehicle using an 800 V charging system; a gear ratio of 13.16 was selected. To analyze whether the

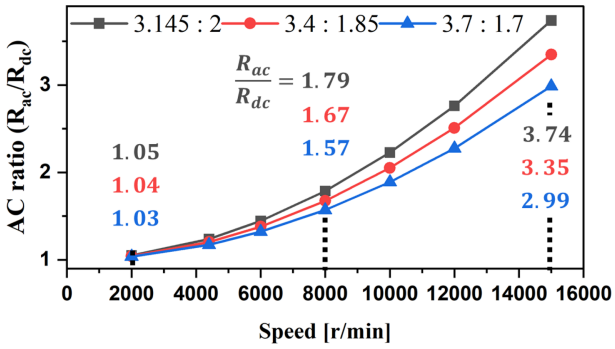

Fig. 2. (Color online) AC resistance ratio by wire aspect ratio.

Table 1. Model's design specifications.

Parameter	Unit	Value
DC Link Voltage (nom.)	V	500~750 (590)
Output power	kW	180
Torque	Nm	350
Max Speed	r/min	15,000
Stator outer diameter	mm	200
Rotor outer diameter	mm	132
Air gap	mm	0.8
Axial length	mm	150

hairpin winding is suitable to design a traction motor for an EV based on the characteristics of AC resistance, modeling was performed using an ANSYS Electronics Desktop, an electromagnetic field finite element analysis program, and a comparative analysis was performed.

Generally, a round wire is used as a motor winding. As shown in Fig. 3, a death space exists between the windings or slots owing to the structure of the round wire. This is because the space in the slot is limited. This is improved by using a rectangular wire for the P2 drive motor. Because the P2 motor should have a small axial length, it is designed as a tooth concentration winding with a short axial end coil length of the motor. In addition, because a split-core structure is possible, the winding process is relatively easy for both round and square wires. Conversely, traction motors for EVs are designed with a long axial length to produce high output because of the limited outer diameter. However, the axial direction has a room based on the existing engine room to replace the engine. In addition, the distributed winding method with low vibration and noise is preferred.

The distributed winding-type motor occupies a significant proportion of the total resistance because the end coil is long in the axial direction. In addition, the slot opening width is narrow compared with the tooth concentration, and applying the divided core is challenging. Therefore, a winding that is easy to manufacture and can have a high slot fill factor is preferable. The hairpin winding used in the current high-voltage system of vehicles can satisfy this condition. In traction motors for EVs, the number of windings per slot that can be manufactured is limited to 6-8 layers owing to the damage to windings. Two parallel branches were used to minimize the circulating current. However, a large number of thin windings should be used to reduce the AC resistance loss owing to high frequencies. Hairpin windings were unsuitable in the system using the existing 356-400 V owing to limited parallel branching. However, to reduce the charging speed of the battery and the cost of high-current devices, Hyundai's Ioniq 5, which was released in 2021, applied the 800 V system, and Porsche also applied the Taycan voltage system to 800 V. Therefore, according to the high voltage in the EV market, traction motors for EVs using hairpin windings are being developed by related companies. The design of motors with high power densities using hairpin windings that can improve slot fill factors has become increasingly common. However, information on the manufacturing technology of hairpin winding is quite limited. Moreover, because of the increase in AC resistance loss owing to the use of the hairpin winding, studies on whether hairpin windings are suitable for application to the current vehicle are limited. Therefore, the comparison and analysis of the characteristics of hairpins and round wires is crucial.

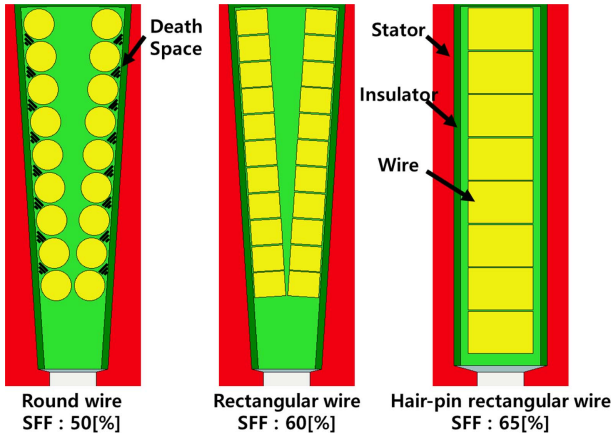

Fig. 3. (Color online) Slot fill factor by wire type.

3.1. AC resistance loss of round wire model

For the round wire model, five strands with a diameter of 1.1 mm were used for the winding size, as shown in Fig. 4. The thickness of the winding was selected within the effective diameter of (4). Theoretically, loss owing to the skin effect rarely occurs. However, when the proximity effect between the coils is considered, some AC resistance

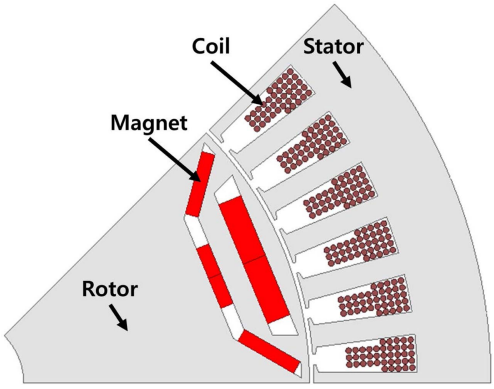

Fig. 4. (Color online) Round wire model.

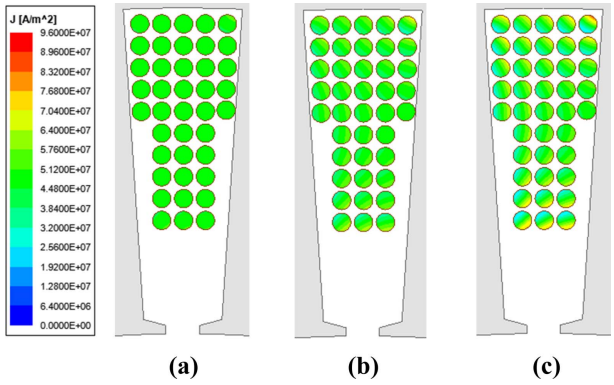

Fig. 5. (Color online) Distribution of the wire's current density according to the operating frequency. (a) Current density distribution at 2,000 r/min. (b) Current density distribution at 8,000 r/min. (c) Current density distribution at 15,000 r/min.

loss occurs as the position of the winding in the slot that influences the actual magnetic path formation changes. The result of analyzing this through ANSYS Electronics is shown in Fig. 5, where the current density distribution in the windings by the operating speed of the round wire model is illustrated.

The FEM simulation analysis results when a sine wave current of 320 Arms is applied at 2,000 r/min (133.33 Hz), 8,000 r/min (533.33 Hz), and 15,000 r/min (1000 Hz) are shown in Fig. 5(a), (b), and (c), respectively. As shown in Fig. 5, unlike (4), which is the ideal formula, the effective area through which the current can pass decreases as the operating speed increases. Consequently, AC resistance loss occurs.

The AC resistance ratio according to the operating speed of the round wire model is shown in Fig. 6. The results indicate that the AC resistance loss can increase according to the proximity effect, shape of the motor, and arrangement of the windings, unlike the theoretically calculated values.

The simulation results of the effective cross-sectional area through which the current can pass through the

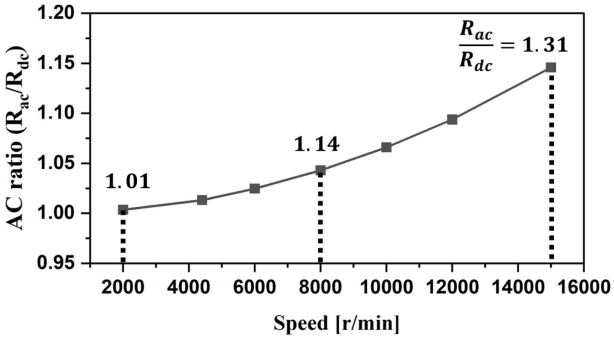

Fig. 6. AC resistance ratio of round wire model.

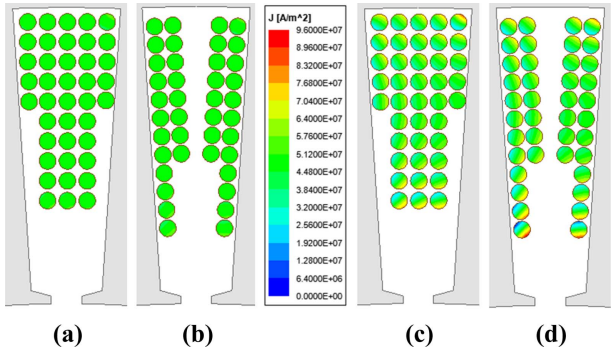

Fig. 7. (Color online) Current density Distribution along the winding distribution pattern. (a) Type A current density distribution at 2,000 r/min. (b) Type B current density distribution at 2,000 r/min. (c) Type A current density distribution at 15,000 r/min. (d) Type B current density distribution at 15,000 r/min.

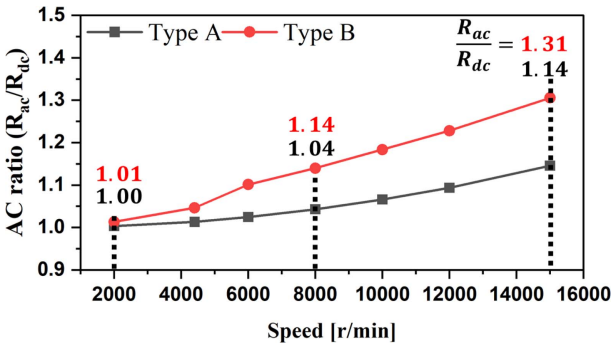

Fig. 8. (Color online) AC resistance ratio by round wire distributed type.

winding according to the distributed winding type are shown in Fig. 7. As shown in Fig. 8, the AC resistance loss owing to the proximity effect can increase depending on the arrangement of the windings. Therefore, in the case of a motor with a high-frequency input power source, the AC resistance loss should be analyzed by understanding the winding distribution in the slot when the motor is manufactured for high-reliability analysis.

3.2. AC resistance loss of hairpin wire model

The shape of the hairpin wire model is shown in Fig. 9. For the hairpin wire, eight layers of 3.4 × 1.85 mm^2 wire were used per slot. AC loss occurs within the driving speed based on (8); however, it differs from the AC resistance ratio in the transient state because the formula considers a simplified shape. The result of analyzing this through ANSYS Electronics and the current density distribution in the winding for each operating speed of the hairpin wire model are shown in Fig. 10.

The FEM simulation analysis results when a sine wave

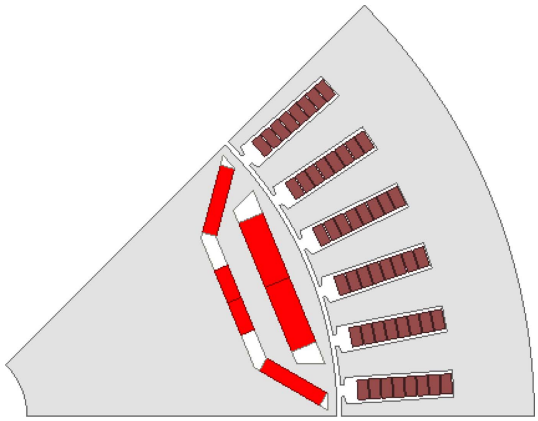

Fig. 9. (Color online) Hairpin wire model.

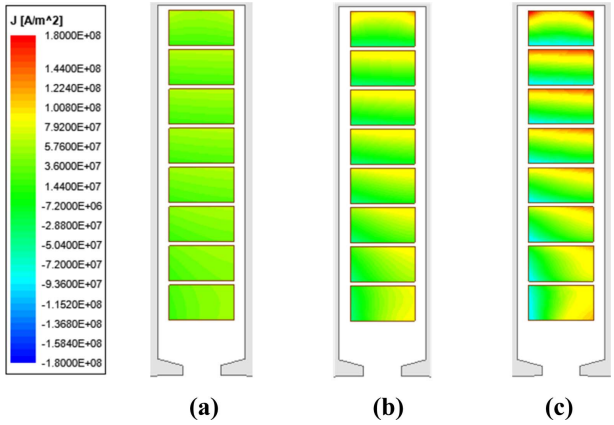

Fig. 10. (Color online) Wire's current density distribution according to the operating frequency. (a) Current density distribution at 2,000 r/min. (b) Current density distribution at 8,000 r/min. (c) Current density distribution at 15,000 r/min.

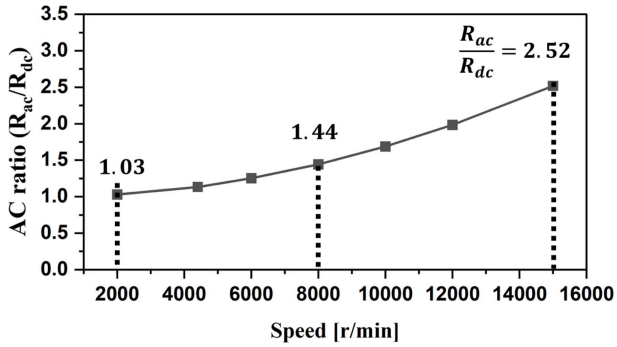

Fig. 11. AC resistance ratio of the hairpin wire.

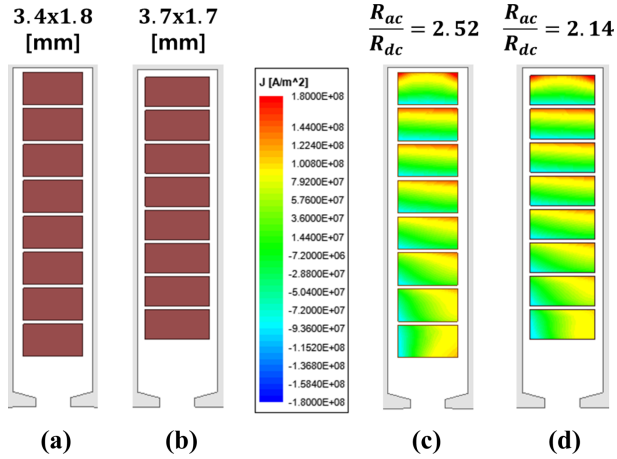

Fig. 12. (Color online) Current density distribution at 15,000 r/min as a function of wire aspect ratio. (a) Winding shape in the slot at α_c=1.83. (b) Winding shape in the slot at α_c=2.18. (c) Distribution of current density at α_c=1.83. (d) Current density distribution at α_c=2.18.

current of 320 Arms is applied at 2,000 r/min (133.33 Hz), 8,000 r/min (533.33 Hz), and 15,000 r/min (1000 Hz) are shown in Fig. 10(a), (b), and (c), respectively. As shown in Fig. 10, the effective area decreases with the same tendency as in Fig. 2 and (8), which is the ideal equation. Consequently, the AC resistance loss increases.

The AC resistance ratio according to the operating speed of the hairpin wire model is shown in Fig. 11. The hairpin wire can have a higher slot fill factor in the slot than when using a round wire, and the DC resistance is designed to be 25.34 % lower than the round wire model. Therefore, a higher slot fill factor is possible in a motor with the same volume; hence, the current density or the output density can be improved. However, in the case of a structure in which windings are dense in the slot, as shown in Fig. 8, AC resistance loss might increase, owing to the skin and proximity effect. Moreover, as seen in (8) and Fig. 2, the AC resistance loss increases as the thickness of the wire increases.

When the aspect ratio of the width b_c and thickness h_c of the winding is defined as $\alpha_c = b_c/h_c$, two models in which the length in the thickness direction is changed in the same winding area are shown in Fig. 12. From the AC resistance loss analysis in Fig. 12, the model with α_c = 1.83 has a larger AC resistance ratio compared with the model with α_c = 2.18.

Thus, the trends shown in (8) and Fig. 2 are shown, and using a wire with a small thickness effectively improves the AC resistance loss.

The actual shape of the hairpin wire is shown in Fig. 13. The hairpin wire is manufactured by twisting the area from ① to ④ in Fig. 13(b) by as much as the width of the next slot pitch. After inserting the manufactured winding into the slot, adjacent wires were welded to ⑤ or ⑥ to connect the windings in series. This structure is called the crown structure. It is effective in reducing the wire thickness to improve AC resistance loss. However, if

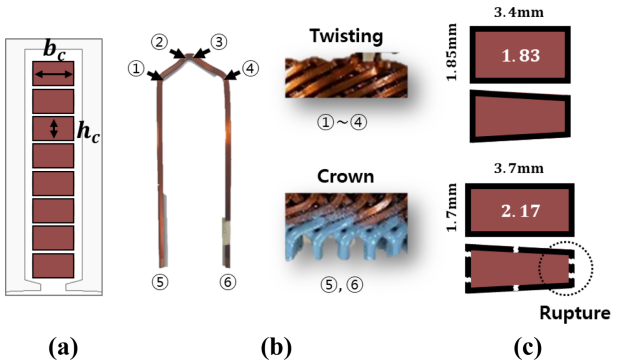

Fig. 13. (Color online) Hairpin wire structure and shape. (a) Wire cross-section. (b) Mold structure of wire. (c) Characteristics according to the wire's aspect ratio.

the wire is deformed into a crown structure for twisting and welding, as shown in Fig. 13(c), the insulating film folds in the direction of the twist. In addition, the insulating film in the outward direction and the wire width become thinner. The insulating film may break if the aspect ratio of these wires is too high, as shown in Fig. 13(c).

Therefore, a design that considers the aspect ratio to prevent breakage is required when designing a motor using a hairpin wire, making AC resistance loss improvement in the high-speed region difficult.

3.3. Comparison of performance for hairpin and round wires

This study compares and analyzes whether the designed motors are suitable for the current EV traction motor design and explains the development direction of the motor based on the analyzed results.

The AC resistance ratio according to the operating speed of the designed motors is shown in Fig. 14. Based on theory and simulation results, the AC resistance loss owing to the skin and proximity effects increases as the input power frequency increases. In the case of a round wire, the AC resistance ratio is close to one because an ideal situation was assumed. However, through the simulation analysis of Fig. 4.4 and Fig. 4.5, additional AC resistance loss may occur, depending on the arrangement of the windings in the slot. According to this result, AC resistance loss should be considered both in hairpin winding motors as well as round and square wires. Definitely, the diameter of the strand can be reduced; however, this will be limited when considering manufacturability, such as the tension and rigidity of the wire.

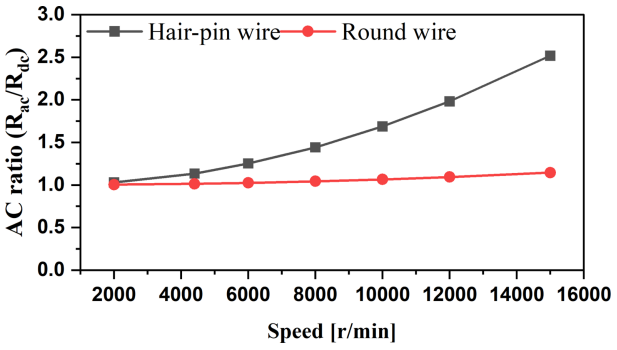

Fig. 14. (Color online) AC resistance ratio by wire type.

When using a hairpin wire, the AC resistance ratio is large compared with that of the round wire model as the operating speed increases. As shown in Fig. 12, the thinner the hairpin wire and the lower the driving speed, the lower the AC resistance loss. Based on the simulation results, Table 1 summarizes the simulation analysis results of the round and hairpin wire models. Both models satisfied the requirements with a required torque of 350 Nm and an output of 160 kW. At the same output density, the current density of the hairpin wire is low, and the resistance of the hairpin wire is 28.36 % lower than that of the round wire. Therefore, the hairpin wire, which can be designed with a high slot fill factor, has a low DC resistance, and the operation efficiency in the low-speed section is higher than that of the round wire. This can be validated from the maximum efficiency in Table 1.

The distribution of the resistance loss when the current to generate the maximum torque at each operating speed of 2,000 and 15,000 r/min is applied to the model is shown in Fig. 15, according to which the DC resistance loss of the hairpin wire model is significantly lower than that of the round wire at low and high speeds. However, because the AC loss at high speeds is large in the hairpin wire, the efficiency in the high-speed region is lower compared with the same output, even when both DC and AC losses are combined.

The efficiency map for each model is shown in Fig. 16. When comparing Figs. 16(a) and (b), the efficiency map of the hairpin wire can use a high slot fill factor;

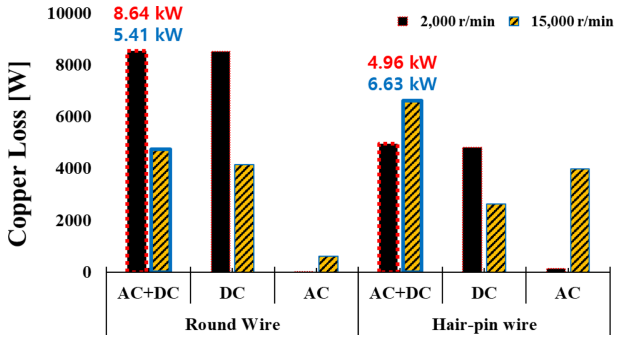

Fig. 15. (Color online) Resistance loss distribution by wire type and operating speed.

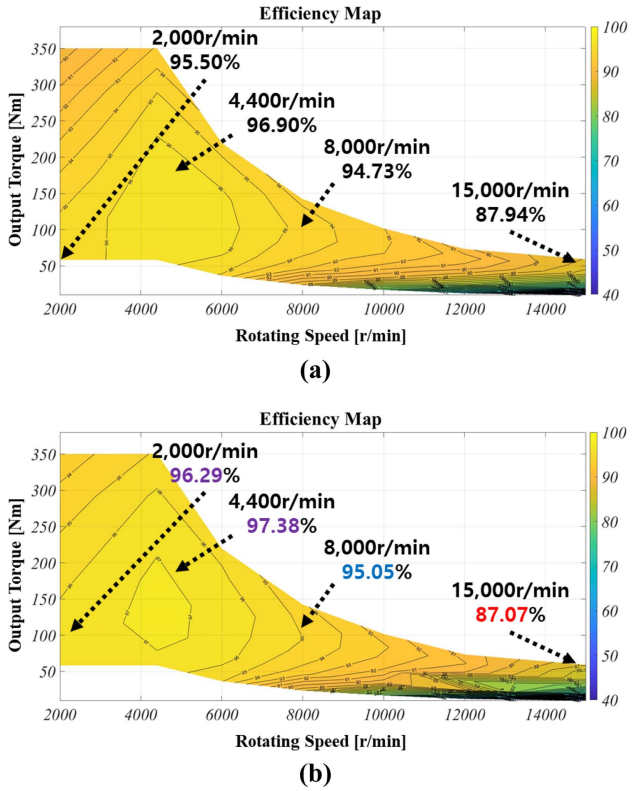

Fig. 16. (Color online) Efficiency distribution by wire type. (a) Round wire model. (b) Hairpin wire model.

therefore, the DC resistance loss is much lower than that of the round wire. In addition, the efficiency is higher than that of the round wire model at medium and low speeds (2,000 to 7,000 r/min), where the loss owing to the skin and proximity effects is small. However, because high AC resistance loss occurs at high speeds, the efficiency is 0.87 % lower at 15,000 r/min.

In the case of an internal combustion engine vehicle, many reviews existed in which the low-speed driving efficiency was poor because the vehicle was designed by citing consumers' preferences for improved fuel efficiency in long-distance driving. Traction motors for EVs can improve driving efficiency at low speeds. If the judgment is based only on the results of Fig. 16, the hairpin wire model with the best driving efficiency at mid-low speed would be suitable if the user mainly drives at mid-low speeds, such as city driving. In the case of a user whose workplace is located outside the city, driving on the highway is more frequent than driving in the city; therefore, the round wire model is preferred for driving efficiency at high speeds.

In addition, considering the manufacturability and satisfactory efficiency in the high-speed operation area, a round wire is appropriate, and considering the high efficiency and cooling performance of the mid-low speed, the hairpin wire is suitable. However, considering the continuous increase in the vehicle's system voltage, we believe that a hairpin wire motor suitable for high-voltage and low-current systems will be preferable for traction motors for EVs in the future.

3.4. Improvement in AC resistance loss

Based on the analysis results, the use of hairpin wires in EV traction motors is predicted to increase. Therefore, studies to effectively improve the AC resistance loss at high speeds, which is a significant problem for hairpin wires, are required.

The aspect ratio of the width and thickness of the hairpin wire were limited because the insulating film could break during the twisting process, as shown in Fig. 13. As shown in Fig. 12, the most effective method of improving the AC resistance loss of the hairpin wire is reducing the thickness of the winding. Therefore, this paper proposes a structure that can prevent damage to the insulating film during the twisting of the winding and

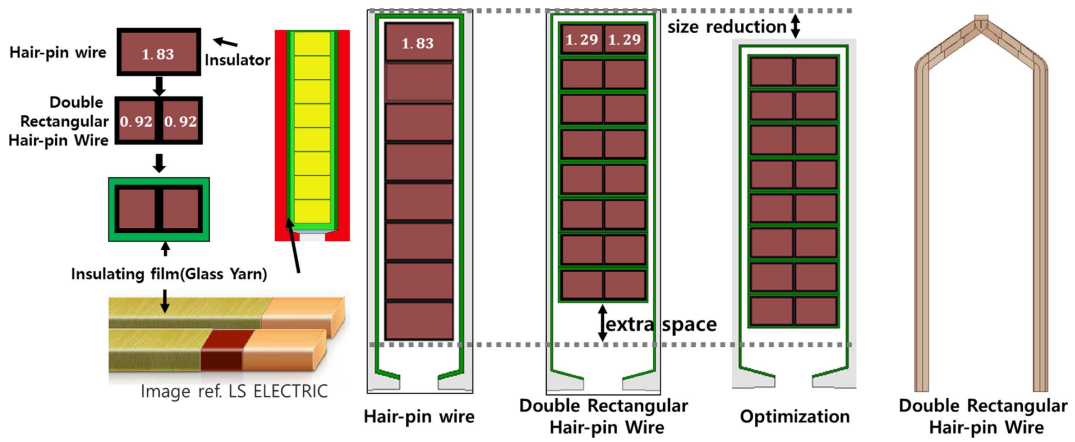

Fig. 17. (Color online) Proposed structure for AC resistance loss improvement.

effectively removes AC resistance loss.

Our proposed structure is manufactured by separating the width direction of the hairpin wire into two stages, as shown in Fig. 17. Each wire was insulated, and a winding structure, in which the insulated wires were fixed with an insulating film, was used. Let the manufactured wire be called a double-rectangular hairpin wire (DR hairpin wire). When the wire is deformed at the same twist angle, the amount of deformation of the insulating film can be improved for the DR hairpin wire, whose aspect ratio is lowered. Therefore, when the DR hairpin wire is used, the thickness direction of the winding can be reduced, and the length in the width direction can be increased more stably than with the conventional hairpin wire. The system voltage of the vehicle is higher, and in the case of the existing hairpin wire, if the outer diameter and axial length of the motor are limited, increasing the number of wires will be challenging. In addition, if a high-grade magnet is not used, the voltage cannot be efficiently used when a voltage of over 800 V is developed.

However, if a DR hairpin wire is used, the length in the thickness direction can be further reduced, and more windings can be used in the extra space in the slot; thus, greater voltage can be used. In addition, the AC resistance loss was effectively reduced. A comparative model was designed, and a simulation analysis was performed using ANSYS Electronics to validate whether the high-speed efficiency of the DR hairpin wire model can be improved compared with that of the hairpin wire model.

The shape of the DR hairpin wire model is shown in Fig. 18. The slot fill factors of the hairpin wire model and the DR hairpin wire model were designed to be the same during fabrication. Through the optimized design, the slot width is wider than that of the hairpin wire, and the length in the direction of the slot is designed to be smaller than

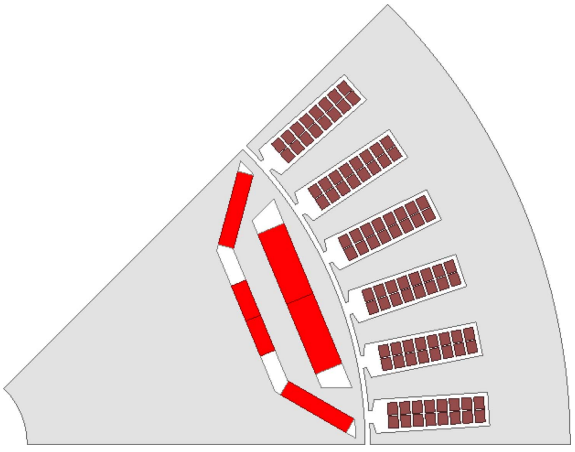

Fig. 18. (Color online) Double-rectangular hairpin wire model.

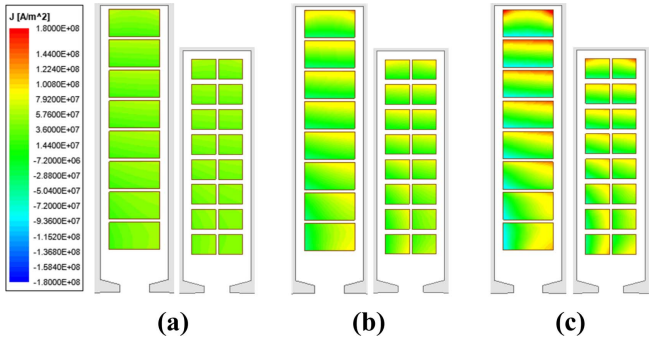

Fig. 19. (Color online) Current density distribution by wire shape. (a) Current density distribution at 2,000 r/min. (b) Current density distribution at 8,000 r/min. (c) Current density distribution at 15,000 r/min.

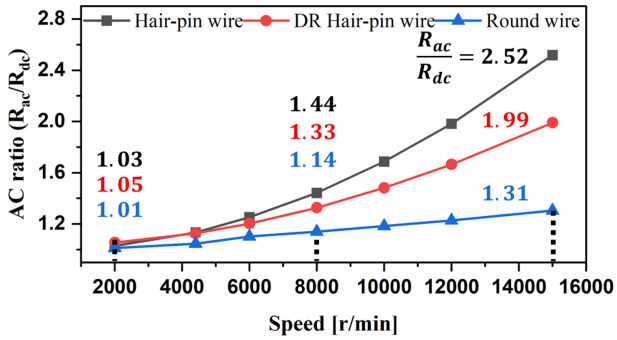

Fig. 20. (Color online) AC resistance ratio by wire type.

that shown in Fig. 19. Fig. 19 shows the FEM simulation analysis results when a sine wave current of 320 Arms is applied to the hairpin and DR hairpin wire models at 2,000 r/min, 8,000 r/min, and 15,000 r/min. As shown in Fig. 19, the current density of the DR hairpin wire model is improved in the high-speed operation range of 15,000 r/min. In addition, in Fig. 20, the AC resistance ratio in the middle- and high-speed operation ranges was significantly reduced from 2.52 to 1.99.

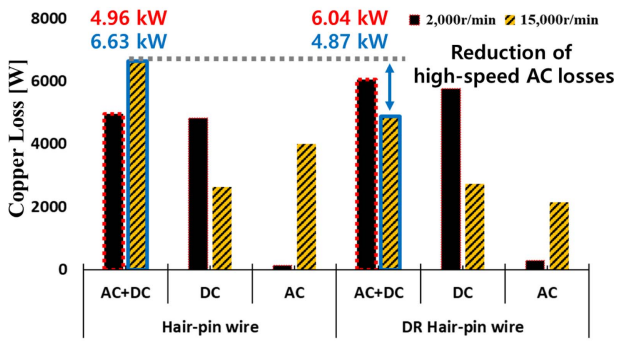

Fig. 21. (Color online) Resistance loss distribution by winding type and operating speed.

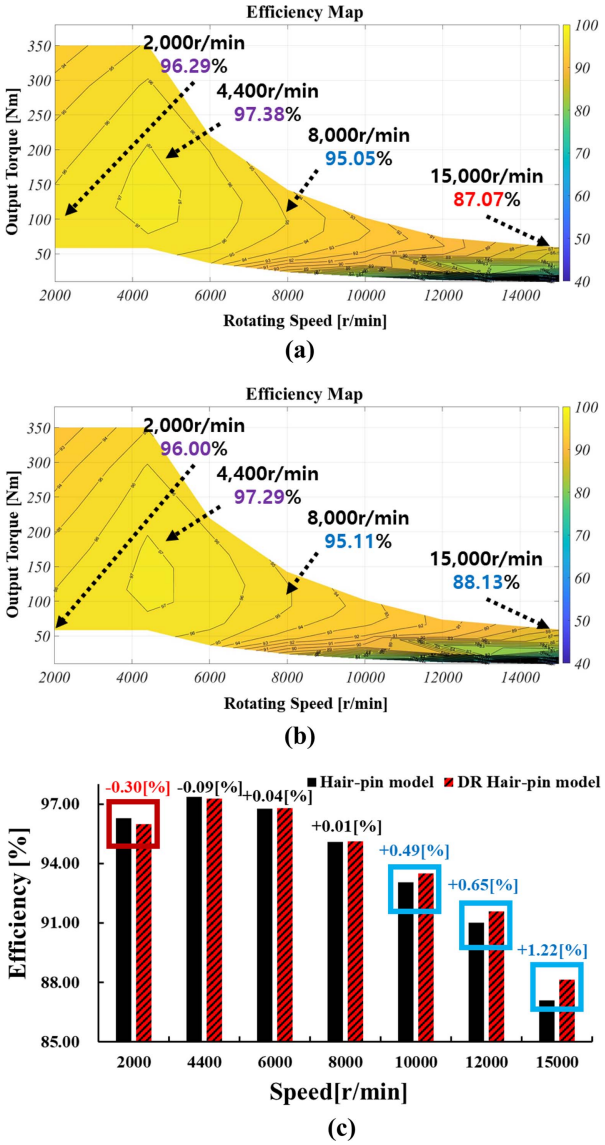

Fig. 22. (Color online) Efficiency distribution by wire type. (a) Hairpin wire model. (b) DR hairpin wire model. (c) Comparison of maximum efficiency.

The distribution of resistance loss according to the operating speed of the hairpin and the DR hairpin wire models is shown in Fig. 21. The DC resistances of the two models were the same; however, the tooth width of the DR hairpin wire model was reduced such that the magnetic flux in the air gap was partially reduced. Therefore, to achieve the target output, approximately 8 % of the current applied was high. The DC resistance loss of the DR hairpin wire model is larger; therefore, the total DC resistance loss at low speeds is higher than that of the hairpin wire model. However, the AC resistance loss is significantly reduced, and the overall resistance loss at high speeds is improved. The efficiency maps of the hairpin and DR hairpin wire models are shown in Fig. 22. As shown in Fig. 22(b), the maximum operating efficiencies of 8,000 r/min and 15,000 r/min in the medium-high-speed operation range were 95.11 % and 88.13 %, respectively. This accounted for approximately a 1.2 % improvement compared with the hairpin wire model. The energy consumption of the vehicle can be significantly reduced by improving the efficiency by 1 %, and high efficiency can be achieved in medium- and high-speed operation when the DR hairpin wire model is used. In addition, Fig. 16 and Table 3 validated that the efficiency in all operation areas is improved compared with the round wire model.

4. Conclusion

Compared with the existing round wire motor, the hairpin wire motor had a disadvantage in that its efficiency was relatively low during high-speed operation. Some companies have already adopted hairpin windings. Thus, this trend is expected to continue. However, the multi-gear method is currently being considered in the single-gear drive system, and improving the AC resistance loss

Table 2. Simulation results obtained based on the model.

Parameter		Unit	Round wire	Hair-pin wire
Pole/Slot		-	8/48	
Max. Torque (2~4.4 kr/min)		Nm	350.19	350.02
Max. Output power (4.4 kr/min)		kW	161.36	161.28
Output power (15 kr/min)		kW	92.96	91.86
Max. Efficiency	2 kr/min	%	95.50	96.29
	4.4 kr/min		96.90	97.38
	8 kr/min		94.73	95.05
	15 kr/min		87.94	87.07
Max. current		A_{rms}	356.52	328.43
Current density		A_{rms}/mm^2	37.52	26.11
DC resistance		Ω	0.02776	0.01988

Table 3. Simulation results obtained based on the model.

Parameter		Unit	Round wire	Hair-pin wire	DB Hair-pin wire
Pole/Slot		-		8/48	
Max. Torque (2~4.4 kr/min)		Nm	350.19	350.02	349.55
Max. Output power (4.4 kr/min)		kW	161.36	161.28	161.06
Output power (15 kr/min)		kW	92.96	91.86	92.03
Max. Efficiency	2 kr/min	%	95.50	96.29	96.00
	4.4 kr/min		96.90	97.38	97.29
	8 kr/min		94.73	95.05	95.11
	15 kr/min		87.94	87.07	88.13
Max. current		A_{rms}	356.52	328.43	338
Current density		A_{rms}/mm^2	37.52	26.11	27.13
DC resistance		Ω	0.02776	0.01988	0.02007

at high speeds in the research direction of traction motors for EVs is crucial. The current 800 V system hairpin wire motor consists of eight layers of windings. However, to drive with a lower current than the current motor, a design with ten layers of wire is required; however, decreasing the thickness of the winding considering the aspect ratio, the defect rate increased. Therefore, studies on materials, such as the DR hairpin wire presented in this study, and studies related to production technology are required.

Acknowledgement

This paper was written with reference to the contents of the master's thesis by the author. And this study was conducted with the support of the National Research Foundation of Korea in 2022, and we are grateful to the relevant ministries (No. 2020R1F1A1075920).

References

[1] B. Sarlioglu, C. T. Morris, D. Han, and S. Li, IEEE Industry Applications Magazine **23**, 14 (2017).
[2] M. Popescu, J. Goss, D. A. Staton, D. Hawkins, Y. C. Chong, and A. Boglietti, IEEE Trans. Ind. Appl. **54**, 2751 (2018).
[3] W. Cai, D. Fulton, and C. L. Congdon, Patent and Trademark Office, U.S. Patent No. 0438429 (2005).
[4] J. Liu, Y. Liang, P. Yang, W. Wang, F. Zhao, and K. Xu, IEEE Access 113403 (2021).
[5] J. Pyrhonen, Design of Rotating Electrical Machines, Wiley, New Delhi (2013).
[6] D. P. Morisco, S. Kurz, H. Rapp, and A. Möckel, IEEE Trans. Magn. **55**, 1 (2019).
[7] G. Berardi, S. Nategh, N. Bianchi, and Y. Thioliere, IECON 2020 The 46th Annual Conference of the IEEE Industrial Electronics Society 815 (2020).
[8] J. H. Moon and M. S. Thesis, Keimyung University, Korea (2022).
[9] C. Du-Bar and O. Wallmark, 2018 XIII International Conference on Electrical Machines (ICEM). 710 (2018).
[10] H. Hämäläinen, J. Pyrhönen, and J. Nerg, IEEE Trans. Magn. **49**, 2967 (2013).
[11] F. Zhang, *et al*., IEEE Transactions on Transportation Electrification **7**, 2914 (2021).
[12] A. Arzillo, *et al*., 2020 International Conference on Electrical Machines (ICEM) 1534 (2020).
[13] M. Vetuschi and F. Cupertino, IEEE Trans. Ind. Appl. **51**, 3068 (2015).
[14] D. Deurell and V. Josefsson, M.S. Thesis, Chalmers University, Sweden (2019).
[15] P. L. Dowell, Proc. IEE. **113**, 1387 (1966).